Structure and photoluminescence of SiC/ZnO nanocomposites prepared by radio frequency alternate sputtering

Yue Zheng · Chunsheng Shi · Naiqin Zhao · Xiwen Du · Jiajun Li

Abstract SiC/ZnO nanocomposites were prepared by radio frequency alternate sputtering followed by annealing in N_2 ambient. Well-crystallized ZnO matrix was obtained after annealed at 750 °C according to X-ray diffractometer patterns. Transmission electron microscopy analyses indicated that the SiC thin layer aggregated to form SiC nanoclusters with the average size of 7.2 nm when the annealing temperature was 600 °C. When the annealing temperatures increased above 900 °C, some of the SiC nanoclusters changed into SiC nanocrystals and surfacial atoms of the SiC nanoparticles were surrounded by a layer of SiO_x ($x \leq 2$) according to the Fourier transform infrared spectrums. The SiC/ZnO nanocomposites annealed at 750 °C exhibit strong photoluminescence bands ranging from 250 to 600 nm. UV light originates from the near band edge emission of ZnO and the blue emission peaked at around 465 nm (2.7 eV) may be due to the formation of emission centers caused by the defects in Si–O network, while the green-emission peak at around 550 nm (2.3 eV) may be attributed to the deep level recombination luminescence caused by the vacancies of oxygen and zinc.

Introduction

In recent years, quasizero dimensional semiconductors or quantum dots have attracted much attention due to their strong photoluminescence (PL) and modified optical properties arising from the quantum confinement effects.

However, these nanoparticles aggregate easily owing to their high surface energy. One of the most effective ways to maintain their individual characteristics is to disperse the nanoparticles into a matrix material. Since the first report by Jain and Lind [1], semiconductor nanoparticles embedded in an insulating matrix have been widely investigated and characterized [2–6].

SiC have excellent physical and electrical properties such as wide band gap, high electrical breakdown field, high thermal conductivity, and saturated electron velocity, making it extraordinary attractive for high temperature and large power applications [7, 8]. In the optical device field, SiC is a potential material for blue LEDs. However, due to its indirect bandgap characteristics, bulk SiC shows weak emission at room temperature [9, 10], which can only emit weak blue light of 480 nm at low temperature. Also, the light-emitting efficiency of the SiC based LED is as low as 1.4×10^{-4} lm/W. It is well known that the emission intensity can be significantly enhanced when the crystallite size diminishes to several nanometers. The SiC nanoparticles have been embedded in an insulating matrix like SiO_2 by several researchers [11, 12]. Being a promising photoelectric material, incorporation of SiC nanoparticle in semiconductor ZnO matrix might be effective to tailor its optical and electrical properties suitable for optical applications. Recently, Zhu et al. synthesized SiC/ZnO nanocomposites by co-precipitation processes and found enhanced UV emission, green emission, and orange emission [13]. Therefore, there is scope to further explore novel synthetic routes for the SiC/ZnO nanocomposites.

In this article, we report the preparation of SiC nanoparticles embedded in ZnO matrix by radio frequency alternate sputtering and a systematic research on their microstructural characteristics and luminescent properties after annealing.

Y. Zheng · C. Shi (✉) · N. Zhao · X. Du · J. Li
Tianjin Key Laboratory of Composite and Functional Materials, School of Materials Science and Engineering, Tianjin University, Weijin Road 92, Tianjin 300072, China
e-mail: csshi@tju.edu.cn

Experimental details

SiC/ZnO multilayer films were deposited on halite and Si(100) substrates by sputtering a ZnO target (60 mm in diameter, 99.99% purity) at 100 W and a SiC target (60 mm in diameter, 99.9% purity) at 50 W alternately using a RF-magnetron sputtering system (JGP-450). The distance between the target and the substrate was 50 mm and base pressure of the deposition chamber was 7.0×10^{-5} Pa. During deposition, the argon pressure was taken at 5.0×10^{-1} Pa and the flow rate of the argon was controlled as 10 SCCM. To prepare the SiC/ZnO multilayer films, a ZnO layer with thickness of 20 nm was deposited on the substrates firstly, and then a SiC layer of 7 nm in thickness was deposited on the top of the deposited ZnO layer. The process was repeated for four times. Finally, a ZnO layer was covered on the top of the sample to terminate the deposition process. The total thickness of the structure obtained was about 130 nm. The as-deposited SiC/ZnO multilayer films were annealed at 400, 600, 750, 800, and 900 °C for 60 min in N_2 ambient. For transmission electron microscopy (TEM) observations, the multilayer films deposited on halite substrates were dipped into de-ionized water to dissolve the substrates and then transferred the films on Mo grids. The structures of the multilayer films annealed at different temperatures were characterized by a Rigaku D/max X-ray diffractometer and an FEI Technai G2 F20 TEM with field-emission gun. Room temperature PL spectra were measured with Hitachi F4500 fluorescence spectrophotometer using an Ar^+ laser excitation source (211 nm) in the wavelength ranges from 250 to 800 nm. The infrared reflection spectra were collected by using a Nicolet 560 Fourier transform infrared (FTIR) spectrometer.

Results and discussion

The X-ray diffraction (XRD) patterns of the SiC/ZnO nanocomposites annealed at different temperatures are shown in Fig. 1. There are mainly five peaks appeared at $2\theta = 31.76°$, $34.42°$, $36.25°$, $47.53°$, and $62.86°$ which correspond to {100}, {002}, {101}, {102}, and {103} planes of the hexagonal ZnO structure, respectively. As the annealing temperature increases, the peaks become sharper and more intense due to the increased particle size as well as the enhanced crystallinity of the ZnO matrix, suggesting that the crystal quality of ZnO matrix is strongly dependent on the annealing temperature. Especially, the {002} peak apparently becomes sharper and its FWHM becomes narrower, indicating that the matrix is becoming c-axis oriented with the annealing temperature increasing up to 750 °C. However, as the annealing temperatures increased
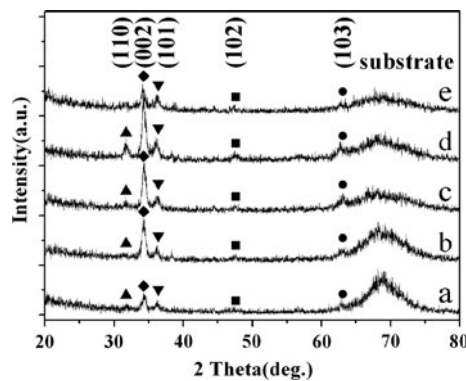

Fig. 1 XRD patterns of the SiC/ZnO nanocomposites annealed at different temperatures. (a) As-deposited, (b, c, d, and e) annealed at 400, 600, 750, and 800 °C, respectively
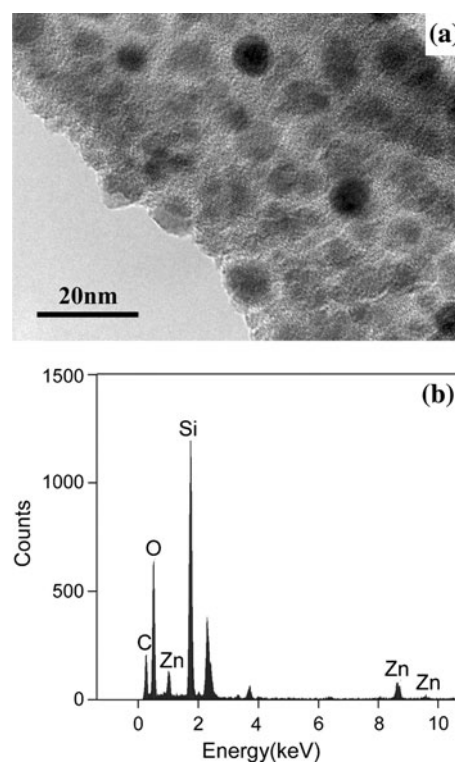

Fig. 2 a TEM image of the SiC/ZnO nanocomposites annealed at 600 °C. **b** EDS pattern of the SiC nanoparticles

above 800 °C, the intensity of the peaks was weakened, which may be attributed to the reduction of ZnO by SiC, leading to the evaporation of Zn at elevated temperatures.

Figure 2a exhibits a typical TEM image of the SiC/ZnO nanocomposites annealed at 600 °C. The average size of the nanoparticles is estimated as 7.2 nm. Energy dispersive X-ray spectroscopy (EDS) analysis performed on the nanoclusters obviously detected Si, O, C, and Zn (Fig. 2b). To modify the structure of the nanoclusters, annealing treatment was carried out at a higher temperature as 900 °C. HRTEM images and the corresponding diffraction

pattern of the selected area of the as-annealed nanoparticles are shown in Fig. 3 in which several well-crystallized nanocrystals are observed. The magnified HRTEM image of one particle (Fig. 3c) revealed the atomic lattice fringes of the nanocrystal clearly and the distance between the fringes was measured as 0.252 nm, which is in agreement to the interplanar distance of {111} planes of 3C-SiC, also known as β-SiC [14].

Figure 3b presents the diffraction pattern of the selected area, which can approve the existence of β-SiC nanocrystals. Therefore, we concluded that the SiC layers aggregated to form amorphous SiC clusters when the annealing temperature was below 800 °C and could not present distinct crystalline peaks in the patterns of XRD. While the annealing temperature increased above 900 °C, some of the SiC nanoclusters began to change into SiC nanocrystals as shown in Fig. 3a.

The FTIR absorption spectra of the SiC/ZnO nanocomposites annealed at 750 and 900 °C are shown in Fig. 4. The peaks at around 740 and 877 cm^{-1} are
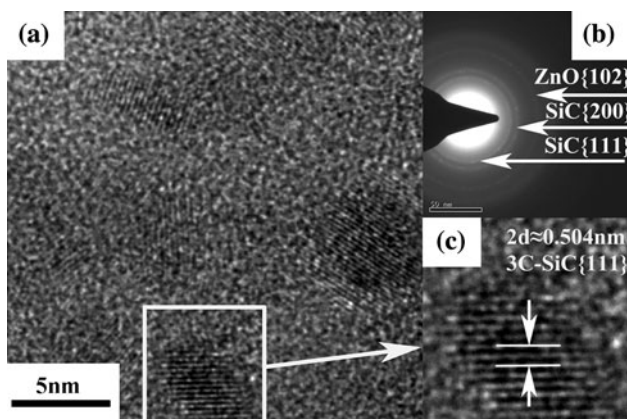

Fig. 3 a HRTEM image of the SiC/ZnO nanocomposites annealed at 900 °C. b Diffraction pattern from the irradiated area. c HRTEM image of one particle. The lattice fringes corresponding to the {111} plane of 3C-SiC can be clearly identified
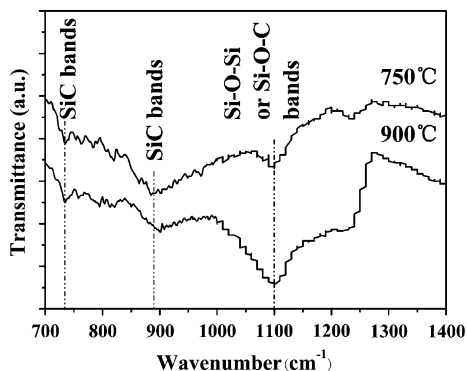
attributed to the SiC stretching modes [15, 16], which means that the C and Si atoms are chemically bonded in these samples. The peak at about 1,100 cm^{-1} corresponds to the Si–O–C or the longitudinal-optical (LO) mode of Si–O–Si linkage [17, 18], which hints the existence of the oxide of the silicon. We concluded that the SiC nanoparticles were surrounded by a layer of SiO$_x$ ($x \leq 2$). The intensities of the Si–O–Si or Si–O–C absorption band increases with the annealing temperature, indicating that more superficial atoms of the SiC nanoparticles were oxidized to SiO$_x$ ($x \leq 2$) owing to the chemical reaction between ZnO and SiC occurring at higher temperature as described by Eq. 1 [19]:

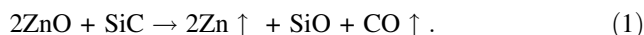$$2ZnO + SiC \rightarrow 2Zn \uparrow + SiO + CO \uparrow. \tag{1}$$

Figure 5 illustrates the PL spectra of the SiC/ZnO nanocomposites annealed at 400, 600, and 750 °C. The peaks at 422 and 633 nm arise from the frequency multiplication of 211 nm excitation. There are two strong emission peaks at around 381 nm (3.3 eV) and 465 nm (2.7 eV) and a weak emission peak at around 550 nm (2.3 eV). The PL emission peaking at around 381 nm (3.3 eV) is the near band edge (NBE) emission of ZnO, because the energy of these peaks is almost equal to the ZnO band gap energy [20]. It is well known that existence of exciton depends on the crystalline quality of the ZnO matrix. In the experiments, we observed that the integrated intensity of PL emission increases with the annealing temperatures, especially after annealed at 750 °C, the intensity of the PL peak increases remarkably, which is in agreement to the result that elevated annealing temperatures could improve the crystalline quality of the ZnO matrix. The intensities of the PL emission peaking at around 465 nm (2.7 eV) and 550 nm (2.3 eV) also strongly depend on the annealing temperature as observed in Fig. 5. In addition, the green-emission peak is attributed to the deep level recombination luminescence caused by the vacancy of oxygen (V_O*) and that of zinc (V_{Zn}) which has been observed frequently by other researchers in preparing

Fig. 4 FTIR absorption spectra of the SiC/ZnO nanocomposites annealed at 750 and 900 °C
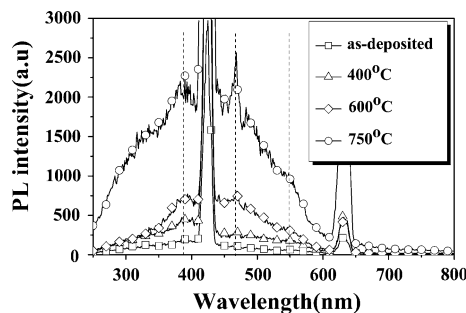

Fig. 5 PL spectra of the SiC/ZnO nanocomposites annealed at different temperatures (*dashed lines* indicate the position of the peaks)

pure ZnO films [21, 22]. The blue-emission peaks at around 465 nm (2.7 eV) is similar to those observed in SiC/SiO$_2$ or Si/SiO$_2$ nanocomposites [11, 12, 23], which may be related to the SiC/SiO$_x$ ($x \leq 2$)/ZnO interface. Chen et al. [11] have detected the PL bands at around 460 nm (2.7 eV) in SiC/SiO$_2$ nanocomposites and they attributed it to two possible reasons: one is the quantum confinement effect of the SiC nanoparticles with small diameters, and the other is triplet-to-ground transition of neutral oxygen vacancies in silicon oxide. In this work, the position of the blue-emission peak keeps unchanged after annealed at different temperatures, so the blue emission was not induced by the quantum confinement effect of the SiC nanoparticles. The peak may be due to the formation of emission centers caused by the related defects in Si–O network at the oxidized outer layers of the SiC nanoparticles, such as –O–Si–O–, –O–Si–C–O–, and neutral oxygen vacancy defects [12]. With the increase of the annealing temperature, more superficial atoms of the SiC nanoparticles will be oxidized to SiO$_x$ ($x \leq 2$), thus more emission centers caused by the related defects in Si–O network will form. Accordingly, the PL intensity of the blue-emission peak increases.

Conclusions

SiC/ZnO nanocomposites were prepared by radio frequency alternate sputtering and then annealed in N$_2$ ambient. The crystallinity of ZnO matrix increased with the increase of the annealing temperature up to 750 °C. The SiC thin layers aggregated to form SiC nanoparticles after annealed at a lower temperature. When the annealing temperature increased, some of the SiC nanoclusters began to change into SiC nanocrystals, but in this case, the ZnO nanocrystals may be destroyed due to the reduction of ZnO by SiC. Meanwhile, the SiC nanocrystals were surrounded by a layer of SiO$_x$ ($x \leq 2$). The films annealed at 750 °C exhibit strong UV PL band at around 381 nm and blue-emission band at around 465 nm, and a weak green-emission band at around 550 nm can also be observed. UV light originates from the NBE emission of ZnO and the blue emission peaked at around 465 nm may be induced by the formation of emission centers caused by the defects in Si–O network, while the green emission peaking at around 550 nm may be attributed to the deep level recombination luminescence caused by the vacancy of oxygen (V_O^*) and that of zinc (V_{Zn}).

References

1. Jain RK, Lind RC (1983) J Opt Soc Am 73:647
2. Canham LT (1990) Appl Phys Lett 57:1046
3. Pal U, García-Serrano J (1999) Solid State Commun 111:427
4. Panda SK, Chakrabarti S, Satpati B, Satyam PV, Chaudhuri S (2004) J Phys D Appl Phys 37:628
5. Pal U, García-Serrano J, Koshizaki N, Sasaki T (2004) Mater Sci Eng B Solid 113:24
6. Cullis AG, Canham LT (1991) Nature 353:335
7. Fan JY, Wu XL, Chu PK (2006) Prog Mater Sci 51:983
8. Shi SL, Xu SJ, Wang XJ, Chen GH (2006) Thin Solid Films 495:404
9. Hoffman L, Ziegler G, Theis D, Weyrich C (1982) J Appl Phys 53:6962
10. Devaty RP, Choyke WJ (1997) Phys Status Solidi A 162:5
11. Chen DH, Liao ZM, Wang L, Wang HZ, Zhao FL, Cheung WY, Wong SP (2003) Opt Mater 23:65
12. Guo YP, Zheng JC, Wee ATS, Huan CHA, Li K, Pan JS, Feng ZC, Chua SJ (2001) Chem Phys Lett 339:319
13. Zhu HY, Yang HB, Du K, Fu WY, Chang LX, Pang XF, Zeng Y, Zou GT (2007) Mater Lett 61:4242
14. Kamlag Y, Goossens A, Colbeck I, Schoonman J (2001) Appl Surf Sci 184:118
15. Sundaram KB, Alizadeh J (2000) Thin Solid Films 370:151
16. Ye H, Zhao JQ, Zhang YH (2004) J Appl Polym Sci 91:936
17. Ma QS, Chen ZH, Zheng WW, Hu HF (2003) Mater Sci Eng A Struct 352:212
18. Lasorsa C, Morando PJ, Rodrigo A (2005) Surf Coat Technol 194:42
19. Eftekhari Yekta B, Marghussian VK (1999) J Eur Ceram Soc 19:2969
20. Reynolds DC, Look DC, Jogai B (2000) J Appl Phys 88:5760
21. Lin BX, Fu ZX, Jia YB (2001) Appl Phys Lett 79:943
22. Liu M, Kitai AH, Mascher P (1992) J Lumin 54:34
23. Son JH, Kim TG, Shin SW, Kim HB, Lee WS, Im S, Song JH, Whang CN, Chae KH (2001) Opt Mater 17:1